Evidence for Formation of the Veratryl Alcohol Cation Radical by Lignin Peroxidase†

Aditya Khindaria, Thomas A. Grover, and Steven D. Aust*

Biotechnology Center, Utah State University, Logan, Utah 84322-4705

Received February 15, 1995; Revised Manuscript Received March 29, 1995®

ABSTRACT: Lignin peroxidases (LiP) catalyze the H_2O_2-dependent two-electron oxidation of veratryl alcohol (VA) to veratryl aldehyde. We present here, electron spin resonance (ESR) evidence for the formation of the one-electron oxidized intermediate, the veratryl alcohol cation radical ($VA^{\bullet+}$). The ESR spectrum of $VA^{\bullet+}$ was first obtained in a fast-flow system with Ce(IV) as an oxidant and 10% HNO_3 to stabilize the radical. This ESR signal was deconvoluted, and the hyperfine splitting constants were determined. The identity of the radical was confirmed by computer simulation of the ESR spectrum and calculation of spin and charge densities on the radical. An identical radical signal was observed with LiP, also in a fast-flow incubation containing 10 μM LiP, 2 mM VA, and 500 μM H_2O_2 at pH 3.5. The Fourier transforms of the ESR signals further confirmed that the spectra obtained with both Ce(IV) and LiP were due to the same radical species. The $VA^{\bullet+}$ had a distinct visible spectrum in 98% H_2SO_4 with an absorbance maximum at 529 nm. The extinction coefficient of the $VA^{\bullet+}$ spectral band at 529 nm was calculated to be 11 000 M^{-1} cm^{-1}. The $VA^{\bullet+}$ was found to be a strong acid, as are other cation radicals, with the pK_a at −1.0 pH. This value was determined by quantitating both the concentration of $VA^{\bullet+}$ by visual and ESR spectrometery and the *g*-value of the ESR signal at various pH values.

Lignin peroxidases (LiP),[1] secreted extracellularly by *Phanerochaete chrysosporium*, are largely responsible for the ability of the white rot fungus to degrade lignin and a variety of environmental pollutants (Bumpus et al., 1985; Barr & Aust, 1994). The catalytic cycle of LiP involves oxidation of ferric peroxidase by two electrons to compound **I**, which oxidizes substrates by one electron leading to the formation of compound **II**. Compound **II** can also oxidize substrates by one electron completing the catalytic cycle of LiP (Tien, 1987; Wariishi et al., 1991). Many organic and inorganic substrates are directly oxidized by LiP (Tien & Kirk, 1984). One of the more important substrates, veratryl alcohol (VA), is a secondary metabolite of the fungus (Lundquist & Kirk, 1978).

Veratryl alcohol is oxidized to veratryl aldehyde by LiP (Tien et al., 1986). It is speculated that VA is oxidized by one electron to the veratryl alcohol cation radical ($VA^{\bullet+}$) (Harvey et al., 1986; Gilardi et al., 1990; Haemmerli et al., 1987), since both compound **I** and compound **II** of LiP are one-electron oxidants (Tien, 1987; Wariishi et al., 1991). Harvey and co-workers (Harvey et al., 1986), who first proposed the formation of this intermediate, have provided NMR evidence for the formation of $VA^{\bullet+}$ during LiP catalysis (Gilardi et al., 1990). This was based on the observation that the peak attributable to the methoxy protons was broadened during oxidation of VA by LiP, possibly due to the formation of a radical species. This, however, could be an artifact of binding of VA to LiP−compound **II**, since a binding step is involved in reduction of LiP-compound **II** to ferric enzyme by VA (Wariishi et al., 1991).

The $VA^{\bullet+}$ is considered an important intermediate in LiP catalysis with roles ranging from an oxidant for LiP−compound **III**, reverting it back to ferric enzyme (Barr & Aust, 1994), to being a redox mediator for indirect oxidations (Harvey et al., 1993). The proposed scheme for this latter role is that VA is oxidized to $VA^{\bullet+}$ by LiP, which acts as an oxidant of a secondary molecule. This is supported by the observation that VA stimulated the oxidation of a number of compounds by LiP (Goodwin et al., 1995; Chung & Aust, 1995a). However, others have provided evidence that VA completes the catalytic cycle of LiP allowing for continued turnover of the enzyme, thus stimulating the oxidation of substrates that cannot reduce LiP−compound **II**, attributing no special role to $VA^{\bullet+}$ (Koduri & Tien, 1994). Still others argue that VA merely prevents the inactivation of LiP by H_2O_2 (Valli et al., 1990).

Thus, in light of the importance of $VA^{\bullet+}$ and the conflicting evidence prevalent in the literature, electron spin resonance (ESR) data would be good evidence for the formation of $VA^{\bullet+}$ during oxidation of VA by LiP. We have been able to detect the $VA^{\bullet+}$ by direct ESR using a fast-flow system. Cerium(IV) was first used as a one-electron oxidant to generate and characterize $VA^{\bullet+}$. Subsequently, we were able to detect the $VA^{\bullet+}$ during the normal catalytic turnover of LiP with H_2O_2. The visible absorption spectrum of the $VA^{\bullet+}$ was characterized. The deprotonation of the $VA^{\bullet+}$ to the neutral radical was investigated using both the visible absorption and ESR spectroscopy.

EXPERIMENTAL PROCEDURES

Materials. Hydrogen peroxide, Tempol, ceric ammonium sulfate, and tartaric acid were purchased from Sigma Chemical Co. Veratryl alcohol was obtained from Aldrich Chemical Co. Prior to use, VA was vacuum distilled to free

† Supported by NIEHS Superfund Basic Research and Training Grant ES04922.

* To whom correspondence should be addressed [telephone (801) 797-2730; FAX (801) 797-2755].

® Abstract published in *Advance ACS Abstracts,* May 1, 1995.

[1] Abbreviations: LiP, lignin peroxidase; VA, veratryl alcohol (3,4-dimethoxybenzyl alcohol); $VA^{\bullet+}$, veratryl alcohol cation radical; ESR, electron spin resonance.

0006-2960/95/0434-6020$09.00/0

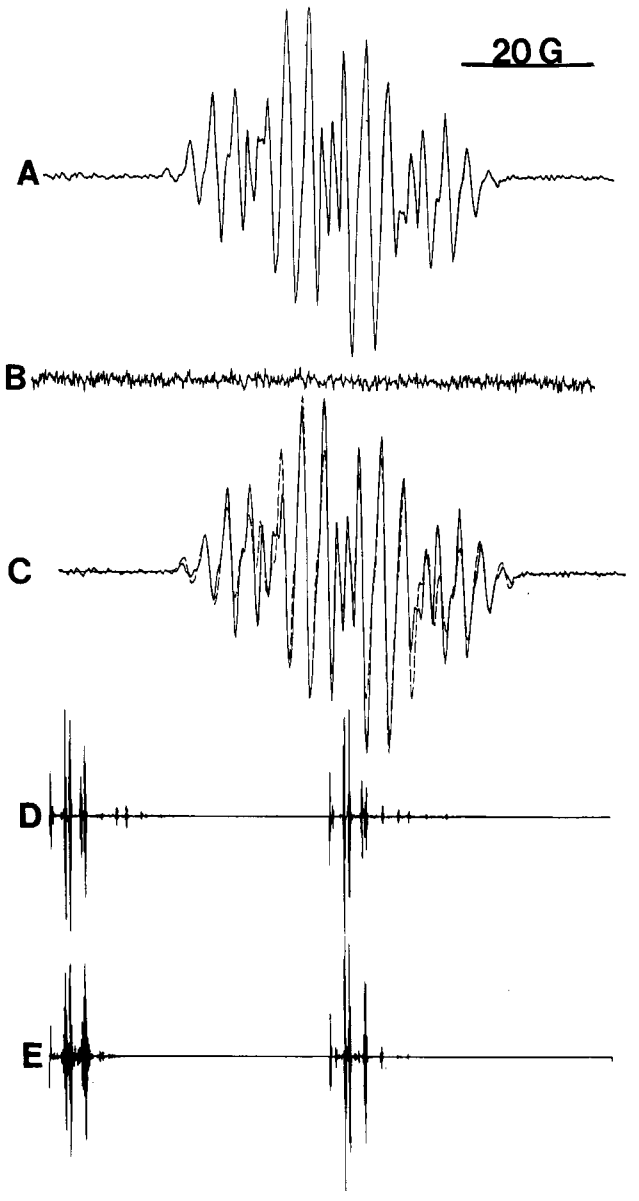

FIGURE 1: Experimental and simulated ESR spectra of $VA^{\bullet+}$ and the Fourier transforms of the ESR spectra. (A) is the ESR spectrum obtained when 10% HNO_3, 2.5 mM Ce(IV), and 2.5 mM VA were reacted in a fast flow incubation (8 mL/min) in a ESR flat cell. B is the spectrum obtained using the same conditions as A except that Ce(IV) was omitted. C is the computer simulation of the ESR spectrum obtained in A (dashed line) superimposed on the experimental spectrum. The hyperfine splitting and other parameters used for the computer simulation are given in Table 1. (D) is the Fourier transform of the spectrum in (A). (E) is the Fourier transform of the simulated spectrum in (C). Spectrometer settings were modulation amplitude 0.4 G, time constant 40 ms, scan time 40 s, microwave power 20 mW, and receiver gain 2×10^4.

it of a trace contaminant (Tien et al., 1986). Sodium succinate, succinic acid, H_2SO_4 (98%), and HNO_3 (68%) were purchased from Mallinckrodt. All chemicals were reagent grade and were used without further purification. All buffers and solutions were prepared using purified water (Barnstead NANOpure II system; specific resistance 18.0 $M\Omega\ cm^{-1}$). Pure lignin peroxidase isozyme H2 ($pI = 4.4$) was used throughout the study and was purified as described previously (Tuisel et al., 1990).

ESR Measurements. All ESR spectra were recorded on a Bruker ECS-106 spectrometer, operating at 9.7 GHz and 50 kHz modulation frequency. A quartz flat cell with a dead volume of 125 μL was used for all measurements. For ESR

Table 1: Coupling Constants for the Protons on $VA^{\bullet+}$ Used for Simulation of the ESR Spectrum[a]

position of protons	coupling constant, a_H (G)	position of protons	coupling constant, a_H (G)
CH_2	6.14	OCH_3 (C_4)	7.76
$C_{2\ ring}$	2.85	$C_{5\ ring}$	3.05
OCH_3 (C_3)[b]	0.49	$C_{6\ ring}$	3.38

[a] Line width, 0.98 G; line shape, 68% Gaussian and 32% Lorentzian. [b] The ring carbon number in parentheses denotes the position of the methoxy group on the ring.

detection of the $VA^{\bullet+}$ generated with Ce(IV) a flow system was used as described previously (Dixon et al., 1973). A 5 mM solution of Ce(IV) was prepared in 20% HNO_3 which was mixed with a 5 mM solution of VA at a flow rate of 8 mL/min. The data for determining the extinction coefficient were also obtained in the above mentioned system except that varying equimolar concentrations of VA and Ce(IV) were flowed together. For the pK_a determination of the $VA^{\bullet+}$ the same equimolar concentrations of VA and Ce(IV) were flowed together at varying pH. The g-values were measured using Tempol ($g = 2.0056$; Knowles et al., 1976). The radical concentration was determined by double integration of the first derivative spectra using Tempol as a standard. Standard solutions of Tempol were prepared using an extinction coefficient of 1440 $M^{-1}\ cm^{-1}$ at 240 nm (Morrisett, 1976). For the detection of $VA^{\bullet+}$ formation by LiP, a two-syringe fast-flow system was used. Syringe A contained 20 μM LiP, and syringe B contained 4 mM VA and 1 mM H_2O_2. The contents of the two syringes were mixed and flowed together at 15 mL/min through the quartz flat cell. The quartz cell had a dead volume of 125 μL.

Visible Absorption Studies. All spectral scans were obtained on a Shimadzu UV-160U spectrophotometer. The $VA^{\bullet+}$ was generated in 98% H_2SO_4 by reacting equimolar concentrations of Ce(IV) and VA.

Computer Simulation. The $VA^{\bullet+}$ ESR spectrum was simulated using the ECS-106 ESR software simulation package. The simulation was optimized using NIEHS simulation software WINSIM (Duling, 1994).

RESULTS

Oxidation of VA with Ce(IV). An ESR signal was detected (Figure 1A), presumably due to $VA^{\bullet+}$, when Ce(IV), VA, and 10% HNO_3 were reacted in a fast-flow system. The acid was added to stabilize the cation radical formed by the oxidation of VA with Ce(IV). The flow rate through the ESR flat cell was 8 mL/min. This radical signal was not detected when Ce(IV) (Figure 1B), VA, or HNO_3 were left out of the reaction mixture or when the pH was raised to 3.5. An ESR spectrum was simulated using the hyperfine splitting constants measured from the experimental spectrum. The individual contributions of the VA protons to ESR hyperfine splittings are presented in Table 1. The magnetic parameters agree well with the literature data for methoxy-substituted aromatic compounds (Kersten et al., 1985; Dixon & Murphy, 1976). These assignments are also supported by the calculated spin and charge densities for the $VA^{\bullet+}$ (Figure 2). These calculations are consistent with what would be predicted from the inductive effect of the methoxy groups. The simulated spectrum obtained from these predictions (dashed line superimposed on the experimental spectrum: Figure 1C) was similar to the experimental spectrum. The Fourier transforms of both the experimentally obtained

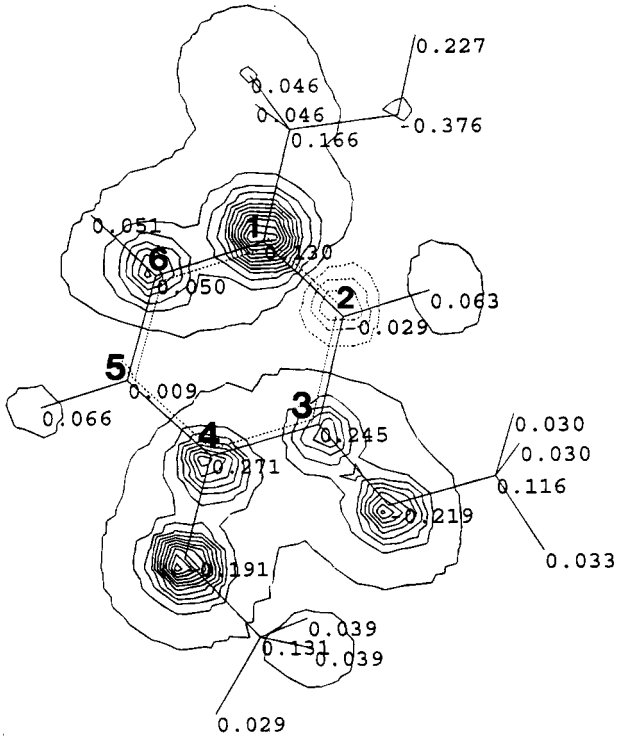

FIGURE 2: Calculated spin and charge densities on $VA^{\bullet+}$. The numbers are the charge densities while the contour plots represent the spin densities. The values were obtained on HyperChem using the selfconsistent field algorithm (PM3) for semiempirical quantum mechanics calculation.

(Figure 1D) and the simulated spectra (Figure 1E) were similar. From these analyses it was concluded that the ESR spectrum was due to $VA^{\bullet+}$.

Formation of $VA^{\bullet+}$ by Lignin Peroxidase. A two-syringe fast flow system was used for the detection of $VA^{\bullet+}$ formed during normal catalytic turnover of LiP. One syringe contained LiP while the other contained VA and H_2O_2. The contents of the two syringes were mixed and flowed together at 15 mL/min, combined flow rate, resulting in a reaction time of 0.5 s in the quartz flat cell (125-μL dead volume). This reaction time was used to ensure that $VA^{\bullet+}$ was not oxidized further by LiP–compound **II** (Harvey et. al, 1993) and was calculated from the known rate constant for the reaction of LiP–compound **I** with VA (Koduri & Tien, 1994). The ESR spectrum of $VA^{\bullet+}$ formed by LiP was detected in a fast-flow incubation system containing 10 μM LiP, 2 mM VA, and 500 μM H_2O_2 at pH 3.5 as shown in Figure 3A. This signal displayed a line width of 1.57 G as compared to 0.98 G for the signal obtained with Ce(IV). This slight broadening of the signal was probably due to the weak interaction of $VA^{\bullet+}$ with the enzyme, leading to either relaxation in the protein lattice or slow tumbling due to the interaction with the relatively large protein molecule. Confirmation of the radical identity was obtained by computer simulation of the ESR spectrum (dotted line superimposed on the experimental spectrum; Figure 3B). The hyperfine splitting constants used for the computer simulation were the same as given in Table 1, except that a line width of 1.57 G was used. The concentration of the $VA^{\bullet+}$ was determined to be 5.9 μM by double integrating the spectrum and using Tempol as a standard. The radical signal was not observed after the flow was stopped (Figure 3C) or when either LiP (Figure 3D) or H_2O_2 (Figure 3E) was left out of

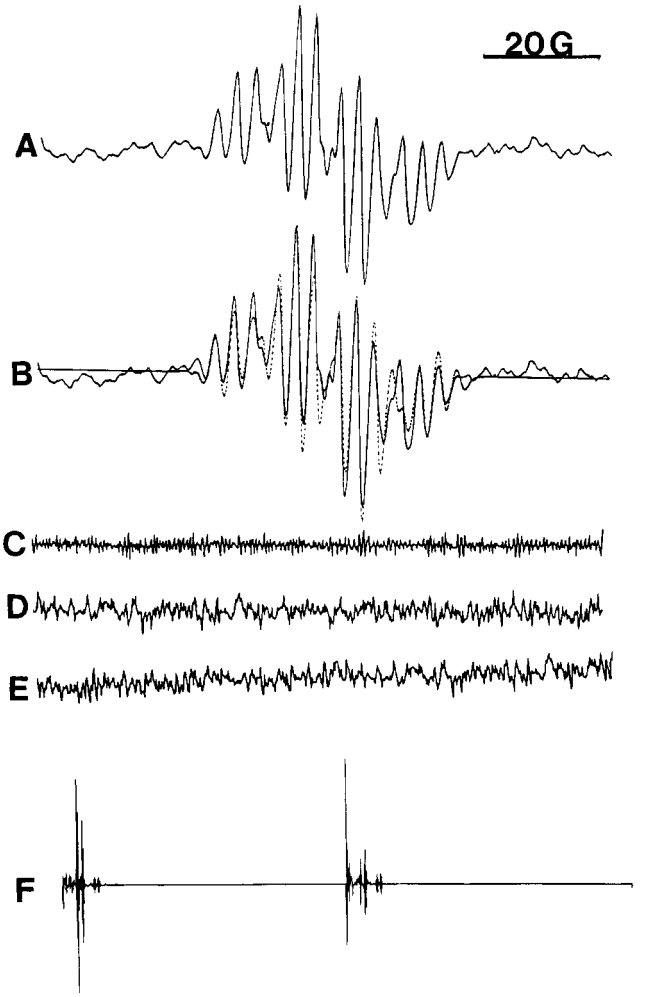

FIGURE 3: ESR spectrum of $VA^{\bullet+}$ obtained during catalytic turnover of LiP, its computer simulation, and Fourier transform. For spectrum A, LiP (10 μM; final concentration) was reacted with VA (2 mM) and H_2O_2 (500 μM) in a fast flow incubation (15 mL/min). Spectrum B is the computer simulation (dotted line superimposed on the experimental spectrum) of the spectrum in (A). The hyperfine splitting constants and other parameters used for the simulation were the same as given in Table 1 except that a line width of 1.57 G was used. Spectrum C was obtained after the flow was stopped in (A). Spectra D and E were obtained using the same conditions as in (A) except that LiP and H_2O_2, respectively, were omitted. Spectrum F is the Fourier transformation of the spectrum in (A). Spectrometer settings were modulation amplitude 1 G, time constant 1310 ms, scan time 80 s, microwave power 20 mW, and receiver gain 2×10^4.

the reaction mixture. The Fourier transform of the radical signal (Figure 3F) further confirmed that the $VA^{\bullet+}$ signal was the same as that obtained with Ce(IV) (Figure 1A).

Visible Spectrum of $VA^{\bullet+}$. The absorption spectrum of $VA^{\bullet+}$ obtained in 98% H_2SO_4 is shown in Figure 4, panel A. To observe the visible spectrum of $VA^{\bullet+}$, the radical had to be stabilized longer than for ESR experiments and was therefore generated in 98% H_2SO_4 by oxidation with Ce(IV). The visible spectrum of $VA^{\bullet+}$ exhibited an absorption maximum at 529 nm which was dependent on the initial concentration of VA (Figure 4, panel A inset). An ESR spectrum similar to the one obtained with Ce(IV) was generated in 98% H_2SO_4 (Figure 4B). The major hyperfine splitting constants of this radical signal were the same as for those shown in Figures 1 and 3. The hyperfine structure of the ESR signal was broadened, possibly due to slow tumbling of the radical cation in the viscous medium (98%

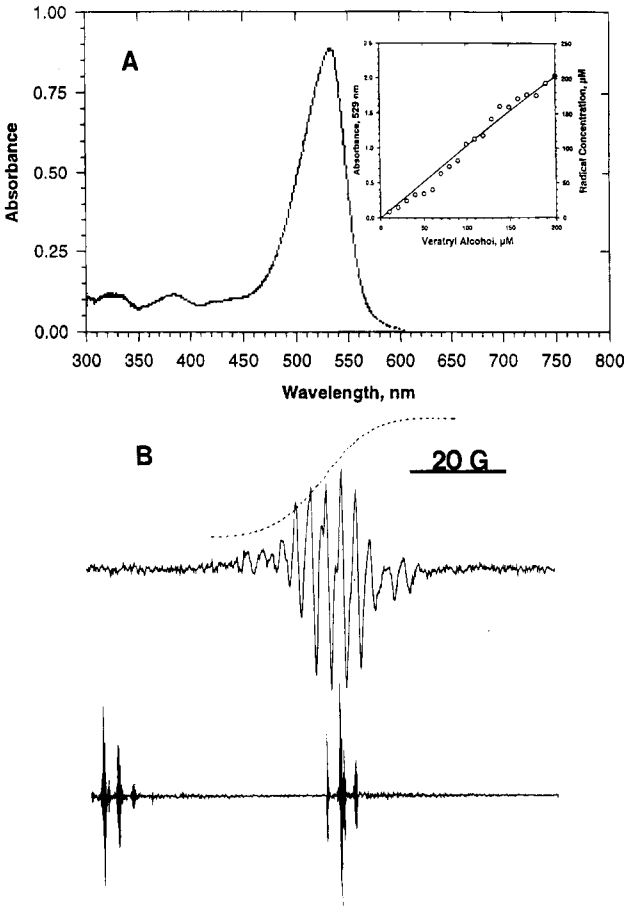

FIGURE 4: Visible spectrum, ESR spectrum, and the Fourier transform of the ESR spectrum of $VA^{\bullet+}$ obtained in 98% H_2SO_4. Panel A shows the absorption spectrum obtained when 75 μM VA was reacted with 75 μM Ce(IV) in 98% H_2SO_4. The inset in that panel shows the concentration dependence of the band at 529 nm on $VA^{\bullet+}$ concentration. The reaction conditions used were the same as above except that varying amounts of equimolar concentrations of VA and Ce(IV) were reacted in 98% H_2SO_4. The concentration of $VA^{\bullet+}$ was calculated from the radical concentration obtained from the ESR spectrum as compared to a Tempol standard (B). The dashed line is the integration of the ESR signal, to get the spin concentration. Further details are provided in the Experimental Procedures. The Fourier transform of the ESR spectrum is also shown.

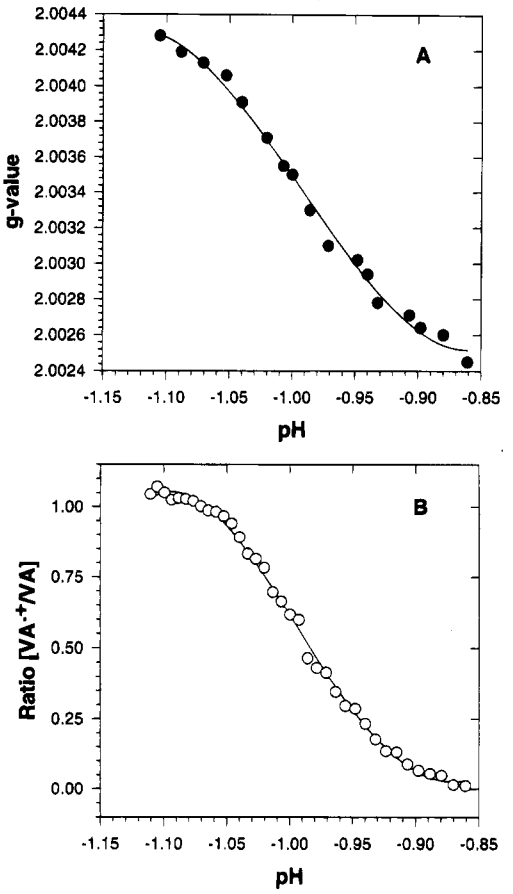

FIGURE 5: The g-value of the ESR signal of $VA^{\bullet+}$ and equilibrium concentration of $VA^{\bullet+}$ as a function of pH. The $VA^{\bullet+}$ was generated in H_2SO_4 of varying pH by oxidation with Ce(IV). Panel A shows the g-value of the $VA^{\bullet+}$ signal as a function of pH. Panel B is the ratio of $VA^{\bullet+}$ to initial concentration of VA plotted as a function of pH. The concentration of $VA^{\bullet+}$ was calculated by both visible absorption spectroscopy using an extinction coefficient of 11 000 M^{-1} cm^{-1} at 529 nm and ESR spectroscopy by comparing the spin concentration to the Tempol standard.

H_2SO_4) and other solvent effects (Knowles et al., 1976). However, the Fourier transform of the ESR signal obtained in 98% H_2SO_4 (Figure 4B) provided strong evidence for the two signals originating from the same radical species. The molar absorptivity of the band at 529 nm was calculated to be of the order of 11000 using the radical concentration obtained from the ESR data. The extinction coefficient was found to decrease with increasing pH, but the λ_{max} was not affected (data not shown).

pK_a of $VA^{\bullet+}$. The pK_a of $VA^{\bullet+}$, generated by oxidation with Ce(IV), was estimated by two methods (Dixon & Murphy, 1976). A solvent of low nucleophilicity (H_2SO_4) was required to suppress deprotonation, allowing for the study of the equilibrium between $VA^{\bullet+}$ and the neutral radical ($VA^{\bullet}$). Advantage was taken of the large change in the g-value of the ESR signal going from the protonated to the neutral species (Bell, 1973; Paul & Long, 1957). This makes the g-value the most useful quantity for determining the pK_a, especially since the centers of spectra could usually be pinpointed even when resolution was poor. The plot of the g-value relative to Tempol versus the pH is shown in Figure 5A. The rate of change of ESR parameters with respect to acid strength is maximum at the pK_a (Kortum, 1965); thus the pK_a corresponds to the inflection point in the plot. A pK_a of -1.0 was determined for $VA^{\bullet+}$ from this plot. Additionally, the equilibria at each pH were calculated by monitoring the concentration of $VA^{\bullet+}$ using both visible absorption and fast-flow ESR spectroscopy (see Experimental Procedures section) and are shown as a plot of pH vs relative concentration of $VA^{\bullet+}$ (Figure 5B). A pK_a also of -1.0 was calculated from this plot, confirming the value obtained with the g-shift method.

DISCUSSION

The results of this investigation clearly demonstrate that $VA^{\bullet+}$ is formed during normal catalytic turnover of LiP. The cation radical is highly acidic as are other cation radicals (Hammerich & Parker, 1984) and is possibly a strong oxidant. Reactivity of $VA^{\bullet+}$ in the chemical system could only be suppressed in solvent systems of low nucleophilicity.

Consistent with the observation that $VA^{\bullet+}$ is very acidic and reactive is the fact that it could be detected only with a fast-flow system. In terms of reactivity, some of the reactions that it can undergo are dimerization, reaction with nucleophiles, electron transfer, and fragmentation (Hammerich & Parker, 1984). To better understand the conditions for maximal stability of $VA^{\bullet+}$, it was first generated

chemically and then characterized. Since LiP essentially catalyzes two one-electron oxidations, we chose the one-electron oxidant Ce(IV) as a chemical mimic of the peroxidase system (Schmidt et al., 1988; Haemmerli et al., 1987). Due to the strong signal intensity, the ESR spectrum of $VA^{\bullet+}$ [generated with Ce(IV)] could be recorded at low modulation amplitude, leading to better resolution which helped assign the coupling constants to the protons. Our ESR assignments are in accord with earlier published literature for oxidation of methoxybenzenes by lignin peroxidase (Kersten et al., 1985).

The ESR assignments are supported by the product profile obtained from oxidation of VA by Ce(IV) by Haemmerli et al. (1987). These researchers reported the formation of a quinone as one of the products following oxidation of VA by Ce(IV). The quinone, 2-methoxy-2,5-cyclohexadiene-1,4-dione, would be expected to form from the attack of water at the C_1 and C_4 positions of $VA^{\bullet+}$ (Figure 2). It is well-known that nucleophiles such as water would attack the most positive center on the radical, and the rate constant for such reaction has been estimated to be higher than 10^7 M^{-1} s^{-1} (Schested & Holcman, 1978). This suggests that the C_1 and C_4 carbons are the predominant sites for the delocalization of the radical, which is consistent with the large coupling constants attributed to the C_1 and C_4 protons. This assignment is also supported by resonance stabilization of the radical by two opposing inductive groups. Another quinone reported to be formed from Ce(IV) oxidation of VA is 2-(hydroxymethyl)-5-methoxy-2,5-cyclohexadiene-1,4-dione, presumably the result of nucleophilic attack on the positively charged C_3 and C_6 positions of the radical (Hammerich & Parker, 1984). The high-spin density on C_6 due to the methoxy group at C_3 would suggest partial delocalization of the radical on this center and a relatively higher coupling constant for the proton as compared to the other ring protons. The methoxy protons would not interact with the free electron due to the lack of an inductive group at C_6. As predicted, the best simulated spectrum was obtained when the C_3 methoxy protons were assigned a small coupling constant of 0.49 G. The formation of ring cleavage products from $VA^{\bullet+}$, resulting from the scission of a carbon−carbon bond, has also been reported (Haemmerli et al., 1987; Schmidt et al., 1988). This is consistent with a ring-delocalized aromatic radical, making the ring protons almost equivalent in terms of coupling constants. These ESR assignments are also supported by the calculated spin and charge densities on $VA^{\bullet+}$ (Figure 2). Furthermore, the Fourier transforms of both the experimental and the simulated spectra were found to be identical, supporting the assignments of the coupling constants.

A strong ESR signal of $VA^{\bullet+}$ was also observed with LiP under normal turnover conditions. The signal width was the same as with Ce(IV) as an oxidant though the line width was larger. The line broadening can be explained by the interaction of $VA^{\bullet+}$ with the protein (Knowles et al., 1976). However, since the line broadening was minimal and the signal width was not affected, the interaction was probably limited to weak electrostatic coupling in the negatively charged active site of LiP (Poulos et al., 1993). This weak interaction would tend to stabilize the $VA^{\bullet+}$ but not significantly constrain the tumbling to affect the resolution of the hyperfine structure. The identity of the radical formed by LiP was confirmed by computer simulation using the same hyperfine constants as used to simulate the spectrum obtained with Ce(IV). Additionally, the Fourier transform of the radical signal recorded with LiP was found to be identical to the Fourier transform of the $VA^{\bullet+}$ signal obtained with Ce(IV). This strongly supports the claim that LiP catalyzes the formation of $VA^{\bullet+}$. This is significant since VA is a secondary metabolite of *P. chrysosporium* (Lundquist & Kirk, 1978), and multiple roles have been proposed for $VA^{\bullet+}$ in LiP catalysis (Barr & Aust, 1994).

Charged aromatic radicals have an absorbance in the visible region of the electromagnetic spectrum. The electronic transition in the lower energy region is due to the presence of an unpaired electron in the highest occupied molecular orbital. Many ring-delocalized cation radicals thus typically absorb visible light over 400 nm (Land et al., 1960). Likewise, $VA^{\bullet+}$ was found to have an absorption maximum at 529 nm in 98% H_2SO_4. The values of λ_{max} and ϵ reported here agree well with those reported in the literature for aromatic cation radicals with similar substituents (Land et al., 1960; Barr & Aust, 1994). It must be mentioned that environmental factors produce detectible changes in λ_{max} and ϵ, so the actual absorbance spectrum of the cation radical under mild conditions may be different. However, the pH of the solvent influences the absorption spectrum only by altering the ionization state of the ionizable chromophores, which would be the case for the cation radical. Thus, though the neutral radical would be expected to have a very different spectrum, the absorbance maximum for $VA^{\bullet+}$ would not be expected to be pH dependent. This was observed, at least in the pH range in which the visible spectrum of $VA^{\bullet+}$ could be recorded. The extinction coefficient, though, was found to decrease with increasing pH. We do not attribute this to the pH dependence of the extinction coefficient but rather to the decreased stability of the cation radical at higher pH due to the higher rate constant for the reaction of H_2O with $VA^{\bullet+}$ and the increased rate of deprotonation (Schested & Holcman, 1978).

Deprotonation of $VA^{\bullet+}$ suggests that it is an acid and exhibits a pK_a value corresponding to the formation of the conjugate base, the neutral radical. The acidities of the cation radicals of aromatic alcohols, phenols, amines, and hydrazines are of magnitudes which allow the direct experimental determination of pK_a values or related parameters (Haemmerich & Parker, 1984). The general approach that has been used in these determinations is to generate the cation radical or the corresponding base, the neutral radical, in solvent systems of differing acidities so that the equilibria can be monitored by UV−visible or ESR spectroscopy. Thus $VA^{\bullet+}$ was generated at several different pH values, and both these spectroscopic methods were used to determine the pK_a value for $VA^{\bullet+}$. Additionally, the g-shift of the radical signal was monitored to determine the pK_a of $VA^{\bullet+}$ (Dixon & Murphy, 1975). The changes in g-value were of the expected magnitude (Barabas et al., 1967) and the pattern of change was similar to that expected from previous work (Bell et al., 1973). This method is immune to the kinetic errors that may be associated with the study of steady-state concentration of the radical. The same, low pK_a value obtained irrespective of the technique strongly points to the acidic nature of $VA^{\bullet+}$. The rate constants for deprotonation of some cation radicals have been reported to be of the order of 10^7 M^{-1} s^{-1} (Eberhardt, 1981). A high rate constant for deprotonation can also be predicted for $VA^{\bullet+}$ due to the active hydroxylmethyl group. In fact, deprotonation and reaction of the carbon-centered neutral radical with molecular

oxygen has been proposed for formation of veratryl aldehyde from $VA^{\bullet+}$ (Haemmerli et al., 1987). However, their data did not allow them to predict the acidic proton on $VA^{\bullet+}$.

From the ESR assignments and the calculated spin and charge densities, it is evident that the methylene protons at C_1 would be the most acidic. Deprotonation would proceed rapidly at physiological pH, resulting in formation of veratryl aldehyde. However, the predicted stoichiometry of two veratryl aldehydes formed per H_2O_2 by the reaction of the neutral radical with O_2 (as two neutral radicals would be formed for one catalytic turnover of LiP) is not consistent with the observed data (Koduri & Tien, 1994). But, if $VA^{\bullet+}$, formed by LiP–compound **I**, is stabilized in the enzyme active site while another molecule of VA is oxidized by LiP–compound **II**, the two could dismutate to give one molecule of VA and one molecule of veratryl aldehyde, consistent with the stoichiometry of one veratryl aldehyde per H_2O_2 that is observed experimentally. Further research is needed before anything definite can be concluded. The stabilization of $VA^{\bullet+}$ within the active site may also explain the low yield of quinones and ring cleavage products formed during LiP oxidation of VA as opposed to Ce(IV) oxidation of VA (Haemmerli et al., 1987). In the former case $VA^{\bullet+}$ would be sheltered in the enzyme active site, while in the latter it would be open to attack by water.

It is also difficult to explain the role of $VA^{\bullet+}$ as a diffusible oxidant due to its short lifetime and rapid rate of deprotonation at the physiological pH. The neutral radical would not be an oxidant while $VA^{\bullet+}$ would not be stable in an aqueous medium at pH 4.5 to mediate electron transfer. This, however, does not preclude the enzyme-stabilized cation radical as a redox mediator. Such speculation is not without reason as some recent studies have provided convincing evidence for this role of $VA^{\bullet+}$ (Goodwin et al., 1995; Chung et al., 1995b). Moreover, redox mediation by cation radicals has been well demonstrated previously (Alder, 1980; Chanon, 1982). The aromatic cation radical would be a strong oxidant. A reduction potential in the range of 1.6 V vs NHE can be predicted from the redox potentials of other cation radicals (Reynolds et al., 1974). This is sufficient to oxidize various lignin model compounds, the proposed natural substrates for LiP. The acidic groups in the vicinity of the proposed VA binding site on the heme edge (Poulos et al., 1993) could stabilize the cation radical. These acidic groups, glutamates 37 and 40, aspartate 183, and the two propionate groups on the heme, are in close proximity and are positioned such that this may be possible. This speculation is supported by the fact that $VA^{\bullet+}$ could be observed at pH 3.5 with LiP but not with Ce(IV) as an oxidant. Also, the radical concentration was lower than the enzyme concentration, suggesting that only enzyme-stabilized $VA^{\bullet+}$ was observed. Conversely, the $VA^{\bullet+}$ generated with Ce(IV) or $VA^{\bullet+}$ that escaped the enzyme active site would be too unstable to be observed. The LiP-stabilized $VA^{\bullet+}$ would serve as an extension of the heme and make the oxidizing equivalents more readily available, especially since the heme in LiP is buried and not accessible to macromolecules such as lignin. Also, the cation radical may be a better oxidant for aromatic chemicals due to the ease of orbital overlap.

In conclusion, we have demonstrated that one-electron chemical and LiP-catalyzed oxidation of VA leads to the formation of $VA^{\bullet+}$. We have been able to characterize the radical and have shown that it is a strong acid and can be a strong oxidant. Further research is needed to fully understand the $VA^{\bullet+}$ and to clarify its role in lignin degradation.

ACKNOWLEDGMENT

We acknowledge Terri Maughan for assistance in the preparation of the manuscript and Yixin Ben for production of LiP. We sincerely thank Dr. IsaoYamazaki, Dr. Vernon D. Parker, and Dr. David Barr for helpful discussions.

REFERENCES

Alder, R. W. (1980) *J. Chem. Soc., Chem. Commun.*, 1184.
Barabas, A. B., Forbes, W. F., & Sullivan, P. D. (1967) *Can. J. Chem. 45*, 267.
Barr, D. P., & Aust, S. D. (1994) *Arch. Biochem. Biophys. 312*, 511.
Bell, R. P. (1973) in *The Proton Chemistry*, 2nd ed., Chapter 3, p 26 Chapman & Hall, London.
Cai, D., & Tien, M. (1992) *J. Biol. Chem. 262*, 11149.
Chanon, M. (1982) *Bull. Soc. Chim. Fr.*, II-197.
Chung, N., & Aust, S. D. (1995a) *Arch. Biochem. Biophys. 316*, 815.
Chung, N., & Aust, S. D. (1995b) *Arch. Biochem. Biophys. 316*, 733.
Dixon, W. T., & Murphy, D. (1976) *J. Chem. Soc., Faraday Trans. 72*, 1221.
Dixon, W. T., Foster, W. E. J., & Murphy, D. (1973) *J. Chem. Soc., Perkin Trans. 2*, 2124.
Dixon, W. T., Moghimi, M., & Murphy, D. (1974) *J. Chem. Soc., Faraday Trans. 2 70*, 1713.
Duling, D. R. (1994) *J. Magn. Reson., Ser. B 104*, 105.
Eberhardt, M. K. (1981) *J. Am. Chem. Soc. 103*, 3876.
Forbes, W. F., & Sullivan, P. D. (1966) *Can. J. Chem. 44*, 1501.
Gilardi, G., Harvey, D. J., Cass, A. E. G., & Palmer, J. M. (1990) *Biochim. Biophys. Acta 1041*, 129.
Goodwin, D. G., Aust, S. D., & Grover, T. A. (1995) *Biochemistry* (in press).
Haemmerli, S. D., Schoemaker, H. E., Schmidt, H. W. H., & Leisola, M. S. A. (1987) *FEBS Lett. 220*, 149.
Hammerich, O., & Parker, V. D. (1984) in *Advances in Physical Organic Chemistry* (Gold, V., & Bethell, D., Eds.) pp 55–189, Academic Press, London.
Harvey, P. J., Schoemaker, H. E., & Palmer, J. M. (1986) *FEBS Lett. 195*, 242.
Harvey, P. J., Gilardi, G.-F., Goble, M. L., & Palmer, J. M. (1993) *J. Biotechnol. 30*, 57.
Kersten, P. J., Tien, M., Kalyanaraman, B., & Kirk, T. K. (1985) *J. Biol. Chem. 260*, 2609.
Knowles, P. F., Mansh, D., & Rattle, M. W. E. (1976) *Magnetic Resonance of Biomolecules*, J. Wiley & Sons, New York.
Koduri, R. S., & Tien, M. (1994) *Biochemistry 33*, 4225.
Kortum, G. (1965) in *Treatise on Electrochemistry*, Chapter 10, p 346, Elsevier, Amsterdam.
Land, E. J., Porter, G., & Strachan, E. (1960) *Proc. Chem. Soc. 84*, 1885.
Lunquist, K., & Kirk, T. K. (1978) *Phytochemistry 17*, 1676.
Morrisett, J. D. (1976) in *Spin Labeling, Theory and Applications* (Berliner, L. J., Ed.) pp 274–338, Academic Press, New York.
Paul, M. A., & Long, F. A. (1957) *Chem. Rev. 57*, 1.
Poulos, T. L., Edwards, S. L., Wariishi, H., & Gold, M. H. (1993) *J. Biol. Chem. 268*, 4429.
Reynolds, R., Line, L. L., & Nelson, R. F. (1974) *J. Am. Chem. Soc. 96*, 1087.
Schested, K., & Holcman, J. (1978) *J. Phys. Chem. 82*, 651.
Schmidt, H. W. H., Haemmerli, S. D., Schoemaker, H. E., & Leisola, M. S. A. (1989) *Biochemistry 28*, 1776.
Tien, M. (1987) *CRC Crit. Rev. Microbiol. 15*, 141.
Tien, M., Kirk, T. K., Bull, C., & Fee, J. A. (1986) *J. Biol. Chem. 261*, 1687.
Tuisel, H., Sinclair, R., Bumpus, J. A., Ashbaugh, W., Brock, B. J., & Aust, S. D. (1990) *Arch. Biochem. Biophys. 279*, 158.
Valli, K., Wariishi, H., & Gold, M. H. (1990) *Biochemistry 29*, 8535.
Wariishi, H., Huang, J., Dunford, H. B., & Gold, M. H. (1991) *J. Biol. Chem. 266*, 20694.

BI9503458